Differential GPS supported navigation for a mobile robot

Jakob Raible, Michael Blaich, Oliver Bittel

HTWG Konstanz - University of Applied Sciences, Department of Computer Science, Brauneggerstraße 55, D-78462 Konstanz, Germany
{jraible,mblaich,bittel}@htwg-konstanz.de

Abstract: The objective of this work is the development of a low cost differential GPS system suited for mobile robotics applications which enhances positioning accuracy compared to a single receiver system. In order to keep costs minimal we used single frequency (L1) receivers, namely U-Blox AEK-4T. We adapted the GPS Toolkit (GPSTk) to work with single frequency (L1) observations in real-time. This allowed us to apply an already existing algorithm, originally intended for Precise Point Positioning (PPP) applications using a double frequency receiver. The core of this algorithm is a Kalman filter that processes code and carrier phase single differences. Carrier phase ambiguities are treated as real (float) values, we do not try to fix them to their correct integer values. In a static test with a baseline length of 11m, observations were collected for five minutes. The developed system achieved a horizontal RMS of 6.9cm. Furthermore we carried out a dynamic test where the rover drove around in a circle. Seven circles were driven in about five minutes. The system determined the circle's radius with an RMS error of 13.2cm.

Keywords: Differential GPS, DGPS, carrier phases, single differences, single frequency, Kalman filter, mobile robots

1. INTRODUCTION

Many outdoor robotics applications require positions that are more accurate than those obtained by a single GPS receiver. Existing RTK-GPS systems already provide accuracies in the sub-centimeter level. However, the geodetic grade double frequency receivers that are usually required for these systems are expensive. Other important factors as size, weight or power consumption limit the possible forms of applications and the acceptance in the field of mobile robotics. Nowadays, inexpensive, small, light and power saving devices exist, but usually they do not provide raw observation data, which is absolutely needed for any differential GPS (DGPS) solution. Some new generation modules promise to bridge this gap by combining the above mentioned factors while remaining inexpensive (U-Blox AEK-4T: €295) and providing raw pseudorange, carrier phase and Doppler observations at an update rate of up to ten Hertz.

This allows the use of these receivers in the context of a scientific application. Especially the carrier phase observation promises to enhance positioning accuracy to a level which should be sufficient for most mobile robotics applications. Compared to existing RTK-GPS solutions that usually use double frequency receivers, the AEK-4T represents a single frequency receiver. This makes the solution of the carrier phase ambiguity problem, involved in carrier phase based DGPS applications, more complicated. Already accomplished research shows that fixing the ambiguities within reasonable time is a problem when inexpensive single frequency receivers and cheap antennas are used (Liu et al. (2003), Pinchin et al. (2008)). Inexpensive receivers and antennas feature high noise levels in the pseudorange observations, which is a problem even for very short baselines. Odijk et al. (2007) examined the popular *LAMBDA* ambiguity resolving algorithm with a single frequency receiver. They conclude that "instantaneous ambiguity resolution based on single-frequency data is only successful with many (> 10) satellites." Takasu and Yasuda (2008) obtained a mean time to first fix with ambiguity resolution of almost eleven minutes for the U-Blox AEK-4T receiver with ANN-MS antenna. Note that losses of lock, which are likely to occur with inexpensive single frequency receivers under dynamic conditions, require the reinitialization of the ambiguities.

Based on these results, we decided to implement a float approach based on Salazar et al. (2008). However, we work with pseudorange and carrier phase single differences at the L1 frequency instead of linear combinations of double frequency observations as presented by Salazar, who worked with double frequency receivers. The solution presented in this paper requires an initialization phase of about four to five minutes. During this period, the positioning accuracy increases. However, the system does not need to be reinitialized after losses of lock or when new satellites are introduced in contrast to single frequency approaches that fix the ambiguities to integer numbers. In our case, positioning accuracy decreases temporary, but quickly reaches an acceptable level when the receiving conditions improve again.

The tests presented in this paper result in a sub-decimeter horizontal RMS error in a static test and a horizontal RMS error of about 13cm in a dynamic test after an initialization phase of five minutes in each case.

2. DIFFERENTIAL GPS BASED ON CARRIER PHASE OBSERVATIONS

The goal of a DGPS system is to enhance positioning accuracy by using two GPS receivers. Usually, one is stationary and its position is exactly known. It is called *reference-* or *base station*. The second receiver whose position is to be determined is called *mobile receiver* or *rover*. A DGPS system enhances the accuracy because the common-mode errors (errors common to both receivers) can be determined and eliminated when the two receivers operate in a limited geographic region. This is usually done by calculating the *baseline vector* (vector between mobile receiver and reference station), where the common-mode errors are canceled out. In order to determine the baseline vector, a classical DGPS system uses the *coarse/acquisition (C/A)* code. By utilizing the carrier signal, on which the C/A code is modulated, the positioning accuracy can be enhanced again.

2.1 Carrier phase observation

Because the discussed method is based on phase observations of the L1 carrier signal (1575.42MHz), a short explanation of the basics of this measurement is provided here according to Odijk et al. (2007). A standard GPS receiver computes its position based on range measurements to the GPS satellites by applying the trilateration technique. These range measurements are usually obtained by tracking the coarse/acquisition (C/A) code. As the name suggests, this code is rather coarse because of its short code length compared to a long chip rate ($\sim$300km/$\sim$300m). The signal propagation delay is obtained by cross correlation between the received C/A code and a replica code generated by the receiver. The coarse nature of the C/A code leads to range measurements that are affected by high noise levels. Especially inexpensive receivers and antennas which are used in this work are affected by this problem. But, in order to track the C/A code, the receiver needs to track the carrier signal as well. This is usually done via phase-locked loop (PLL) filters, which enable the receiver to compute the so called phase ranges. Because of the short wavelength of the L1 signal ($\sim$19cm), these ranges are very precise and characterized by low noise levels. The problem is that the phase ranges are offset to the C/A code ranges by an ambiguous number of whole phase cycles. One can imagine this problem when trying to read from a measurement tape, but only a small area is visible around the measuring point. For example, you would read 47,3cm but you do not know if it is 47,3cm or 147,3cm or even 1047,3cm. The phase range Φ [m] can be described mathematically as follows:

$$\Phi(t) = \rho(t) + c\left(\tau_r(t) + \tau_s(t)\right) + \lambda_1 N' \qquad (1)$$

where

$\rho\,[m]$	true geometric range between satellite and receiver
$c\,[m/s]$	speed of light
$\tau_r,[s]$	receiver clock error
$\tau_s,[s]$	satellite clock error
$\lambda_1,[m]$	L1 wavelength ($\sim$ 19cm)
$N' \in \mathbb{R},[cycles]$	Carrier phase float ambiguity

In fact, the carrier phase float ambiguity term N' consists of three components:

$$N' = \Phi_s(t_0) - \Phi_r(t_0) + N \qquad (2)$$

Where $\Phi_s(t_0)$ is the satellite offset in cycles at initial time t_0 and $\Phi_r(t_0)$ the receiver offset, respectively. $N \in \mathbb{N}$ is the unknown initial number of whole carrier phase cycles between satellite and receiver. Because we do not try to fix N to an integer number, we stay with the term N' as presented in Gao (2006).

Once the ambiguity problem is completely solved, which means that the exact integer number of whole phase cycles between satellite and receiver is known, accuracies in the sub-centimeter level can be reached. Such a system is most commonly referred to as *Real Time Kinematic GPS (RTK-GPS)* or *Carrier Phase Enhancement GPS (CPGPS)*. Usually, these systems use geodetic grade double frequency receivers. This is needed in order to be able to fix the ambiguities to the correct integer values within short time. As stated in section 1, the ambiguity resolution is not possible within short time in our case. Therefore, we float the ambiguities in this approach. This means that the accuracy will not reach the sub-centimeter level but should stay in the decimeter or centimeter level.

As the double differences that are usually applied in RTK-GPS systems achieve their full potential only when fixing the ambiguities to integer values, which we are not doing here, we decided to work with single differences to simplify matters. Thus, we do not have to select a master satellite which would introduce the hand-over problem and additional measurement noise when obtaining the double differences.

2.2 Kalman filter design

Our approach is based on the well-known Kalman filter. A good introduction to the filter is given in Welch and Bishop (1995). The design of the filter that we use for our approach is presented in the following section.

System model   The Kalman filter is trying to estimate the state vector x_t, which describes the system. The state vector of our system has the following form:

$$x_t = \begin{bmatrix} \Delta b \\ \tau_{m,r} \\ N_{m,r}^{'1} \\ \vdots \\ N_{m,r}^{'n} \end{bmatrix} \qquad (3)$$

The symbol Δb represents the baseline vector change compared to the last epoch. The baseline vector is given in a local north (N) east (E) up (U) system. Thus, it consists of the three components ΔN, ΔE and ΔU. Because we work with single differences, the combined receiver clock error $\tau_{m,r}$ of the mobile (roving) receiver m and the reference (base) station receiver r does not cancel out. Therefore, we have to estimate this error. $N_{m,r}^{'i}$ are the float phase ambiguity estimates of the i-th satellites, which are received by both the mobile receiver and the reference station.

The system state for the current epoch t is predicted as follows:

$$\hat{x}_t^- = A\hat{x}_{t-1} \tag{4}$$

Where A is the system state transition matrix, $\hat{x}_t$ the estimate of the system state x and $\hat{x}_t^-$ the predicted system state, which is not yet updated by the measurements. While we assume a white noise model for the change of the baseline vector b and for the combined receiver clock error $\tau_{m,r}$, the combined phase ambiguities N' are treated as constants. Besides the white noise model, we also investigated a random walk model for the change of the baseline vector.

The initial phase ambiguities are determined by subtracting the code observations from the carrier phase observations. This is also the case when the ambiguities need to be reinitialized due to cycle slips or complete losses of lock. Cycle slip detection is a problem for single frequency receivers. We compare the bias between code and phase observations with a computed mean bias in order to decide whether a cycle slip occurred or not. Additionally, the loss of lock indicator (LLI), which is set by the receiver is used to guide this decision. When a cycle slip is detected, the phase ambiguity N' is not projected into the next epoch but it is initialized again, as mentioned above. Because the phase observations are characterized by considerably less noise compared to the code observations, a weight factor is implemented to benefit from this advantage. We weight the phase observations 100 times higher, based on the fact that we assume $\sigma = 1m$ for code observations and $\sigma = 1cm$ for phase observations. Matrix A depends on the model that is applied to describe the position components of the process noise covariance matrix Q. If we apply the white noise model, the last position state $\hat{x}_{t-1}$ is not projected into the estimated new a priori state $\hat{x}_t^-$. Thus, the corresponding elements of A are 0:

$$A = \begin{bmatrix} \mathbf{0} & 0 & \dots & 0 \\ 0 & 1 & \dots & 0 \\ \vdots & \vdots & \ddots & \vdots \\ 0 & 0 & \dots & 1 \end{bmatrix} \tag{5}$$

In contrast, if the random walk model is applied, the position components of A are 1:

$$A = \begin{bmatrix} \mathbf{1} & 0 & \dots & 0 \\ 0 & 1 & \dots & 0 \\ \vdots & \vdots & \ddots & \vdots \\ 0 & 0 & \dots & 1 \end{bmatrix} \tag{6}$$

This means that the last state estimation is used to predict the new a priori state, which corresponds to a "walking" rover that cannot jump in contrast to the white noise model.

Measurement model   The measurement model of our Kalman filter is described by the following equations:

$$\Delta P_{m,r}^i = \Delta P_m^i - \Delta P_r^i \tag{7}$$
$$= \Delta b e^i + c\tau_{m,r} \tag{8}$$
$$\Delta \Phi_{m,r}^i = \Delta \Phi_m^i - \Delta \Phi_r^i \tag{9}$$
$$= \Delta b e^i + c\tau_{m,r} + \lambda_1 N_{m,r}' \tag{10}$$

Where $\Delta P_{m,r}^i$ is the single differenced pseudorange pre-fit residual to satellite i, which is obtained by subtracting the pseudorange pre-fit residual of the reference station ΔP_m^i from the pseudorange pre-fit residual of the mobile receiver ΔP_r^i. Accordingly, $\Delta \Phi_{m,r}^i$ represents the single differenced carrier phase pre-fit residual. In our case, the pre-fit residuals are obtained by subtracting the computed ranges to the satellites from the according pseudorange observations. We calculate the ranges to the satellites based on the computed position of the mobile receiver in the previous epoch and subtract it from the pseudorange observations of the current epoch. This equates to the movement Δb of the mobile receiver in the directions of the the line-of-sight (LOS) unit vectors e^i since the last epoch. The LOS vectors point from the mobile receiver to the satellites. By forming single differences (between mobile receiver and reference station), the common-mode errors such as the satellite clock error and ionospheric and tropospheric delays are canceled out. However, the combined receiver clock error $\tau_{m,r}$ is still existent in the residuals, as described by equations (8) and (10). The single differenced carrier phase residual $\Delta \Phi_{m,r}^i$ additionally contains the differenced (between mobile receiver and reference station) number $N_{m,r}'$ of carrier phase cycles.

The measurement vector z_t looks as follows:

$$z_t = \begin{bmatrix} \Delta P_{m,r}^1 \\ \Delta P_{m,r}^2 \\ \vdots \\ \Delta P_{m,r}^n \\ \Delta \Phi_{m,r}^1 \\ \Delta \Phi_{m,r}^2 \\ \vdots \\ \Delta \Phi_{m,r}^n \end{bmatrix} \tag{11}$$

The vector's length depends on the number n of satellites simultaneously received by the mobile receiver and the reference station.

The measurements z_t can be obtained from the system state x_t as follows:

$$z_t = H_t x_t \tag{12}$$

Where the filter's measurement matrix H_t corresponds to the GPS geometry matrix, which relates the system state x_t to the measurements z_t and looks as follows:

$$H_t = \begin{bmatrix} e^1 & c & 0 & 0 & \dots & 0 \\ e^2 & c & 0 & 0 & \dots & 0 \\ \vdots & \vdots & \vdots & \vdots & \ddots & \vdots \\ e^n & c & 0 & 0 & \dots & 0 \\ e^1 & c & \lambda_1 & 0 & \dots & 0 \\ e^2 & c & 0 & \lambda_1 & \dots & 0 \\ \vdots & \vdots & \vdots & \vdots & \ddots & \vdots \\ e^n & c & 0 & 0 & \dots & \lambda_1 \end{bmatrix} \tag{13}$$

Again, n denotes the number of satellites received by both receivers. As in the measurement vector z, the upper half is related to the single differenced pseudorange pre-fit residuals and the lower half to the single differenced phase range pre-fit residuals. The ones on the main diagonal in the lower right part apply the phase ambiguities N'.

Implementation We implemented our approach in C++ using the *GPS toolkit (GPSTk)*, an open source library and suite of applications for satellite navigation purposes (Tolman et al. (2004)). Because the GPSTk is intended for post-processing applications using double frequency receivers, we had to implement an online converter, that translates the raw observations from the proprietary U-Blox protocol to the RINEX based classes contained in the GPSTk prior to the development of the application itself. After that, we were able to modify an existing class which was originally intended for the use in *Precise Point Positioning (PPP)* applications which use a single geodetic grade receiver, as presented in Salazar et al. (2008).

Our development and testing setup consisted of two Asus Eee PC 901 running Ubuntu Eee, which is an Ubuntu 8.04 Linux derivative adapted to the Eee PC hardware.

The communication link was established through a WLAN Ad-Hoc network. The rover PC was running the application, accessing the base station receiver through *socat*, a linux command line multi purpose relay tool. We were also able to establish a link using a mobile phone which enables our system to be used for applications that involve far ranges between base station and rover. The base station PC was connected to the Internet via conventional broadband access. The rover PC established a dial-up GPRS connection via Bluetooth and accessed the base station receiver through socat, as explained before.

3. EXPERIMENTAL EVALUATION

We carried out a static and a dynamic test to determine the positioning accuracy of our DGPS application.

3.1 Static test

First, we installed a static test setup to determine the positioning accuracy of the discussed system. For this purpose, a parking lot in the industrial area of Constance, Germany was chosen. While only surrounded by humble buildings and small trees, it offers good receiving conditions. The lines of the parking lots and, for the orientation Google Earth, helped us to determine the reference position of the mobile receiver with a measuring tape:

- Easting: 11.0m
- Northing: -0.05m

It should be stated here, that an error of approximately five centimeters is possible when using this method for determining the reference position.

We used the active patch antennas U-Blox ANN-MS that ship with the AEK-4T evaluation kits. Because these antennas work better when installed on a metal plate, we put the antennas on a 25cm x 25cm ordinary steel plate in both tests.

The raw observation update rate was set to 10Hz, which is the maximum of the AEK-4T receivers. We collected observations for ten minutes, this corresponds to 6000 epochs. During this test, six satellites were received by both the reference station and the mobile receiver. The GDOP *(geometric dilution of precision)* value ranged between 3.12 at the beginning and 2.95 at the end. Because

we are not interested in the calculated height information, we do not present this information here. The statistical results only contain horizontal information, RMSE is therefore the horizontal RMS error.

Because our approach focuses on mobile robotics applications, we modeled the process noise Q_t of the Kalman filter as random walk with different models for horizontal and vertical movement. We chose a process spectral density $\frac{\Delta\sigma^2}{\Delta t}$ of $5\frac{m^2}{s}$ for horizontal movement and $1\frac{m^2}{s}$ for vertical movement. The smaller value for vertical movement was chosen based on the fact that a mobile robot usually drives on flat grounds, meaning small vertical movement. We also investigated a white noise model with $\sigma = 100m$. This corresponds to a fully kinematic system, also suitable for airborne applications. The results achieved with this model are almost equal to the random walk approach, which performed slightly better. The positioning error over time using the random walk model is presented in figure 1
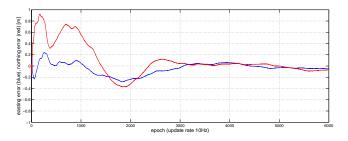

Fig. 1. Static test: Easting (blue) / Northing (red) error in meters over ten minutes of static observation at an update rate of ten Hertz. Process error Q_t as random walk with horizontal $\frac{\Delta\sigma^2}{\Delta t} = 5\frac{m^2}{s}$ and vertical $\frac{\Delta\sigma^2}{\Delta t} = 1\frac{m^2}{s}$.

The statistical results are presented in table 1.

Table 1. Statistical results of static test

	Easting	Northing
Without initialization phase (Epochs 0 - 6000)		
RMSE [m]	0.110	0.298
STD [m]	0.102	0.282
Minimum [m]	10.719	-0.421
Maximum [m]	11.240	0.873
With initialization phase (Epochs 3001 - 6000)		
RMSE [m]	0.037	0.044
STD [m]	0.037	0.044
Minimum [m]	10.949	-0.141
Maximum [m]	11.063	0.002

3.2 Dynamic test

For the dynamic test we attached the rover, a radio controlled model car, to a fix pile using a leash. The rover was able to move in a circle with a known radius. The base station's antenna was mounted on the pile at the center of the circle. A radius of 5m was measured using a measurement tape. Thus, the calculated baseline length should always match this radius. Because we were only interested in the two-dimensional positioning accuracy, we calculated the euclidean distance d as follows:

$$d = \sqrt{\Delta E^2 + \Delta N^2} \qquad (14)$$

Where ΔE is the easting component and ΔN the northing component of the baseline vector obtained by the presented DGPS system. During this test, 5740 epochs were collected at an update rate of 10Hz. The rover was standing still for four minutes at the beginning. This is regarded as initialization phase. Thus, the results of the first 2400 epochs are not incorporated in the statistical results. During the remaining 3340 epochs, the rover was moving in circles at a roughly constant velocity. Seven complete circles were accomplished during this time which yields to an average of 48 seconds per circle. In this test, we modeled the process noise Q_t as white noise with $\sigma = 100m$. Again, we obtained almost the same results using the random walk model with horizontal $\frac{\Delta\sigma^2}{\Delta t} = 5\frac{m^2}{s}$ and vertical $\frac{\Delta\sigma^2}{\Delta t} = 1\frac{m^2}{s}$. Figure 2 shows the computed track.
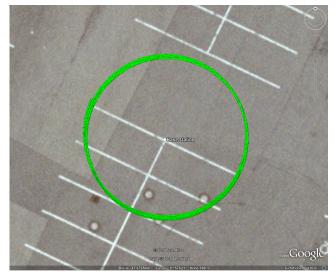

Fig. 2. Dynamic test: Position plot of the dynamic test (all 7 circles)

The statistical results are presented in table 2.

Table 2. Statistical results of dynamic test

	All 7 circles	Last circle
Mean [m]	5.009	5.011
RMSE [m]	0.132	0.084
STD [m]	0.131	0.084
Minimum [m]	4.712	4.876
Maximum [m]	5.271	5.134

Additionally, we determined the center of the circle through circle fitting in a least-squares sense according to Gander et al. (1994). The results are presented in table 3.

Table 3. Circle center obtained through circle fitting

	All 7 circles	Last circle
Easting [m]	0.097	0.114
Northing [m]	0.131	0.037

3.3 Challenging conditions

Because perfect receiving conditions cannot be assumed for every outdoor robotics application, the performance of the presented system was investigated under difficult receiving conditions, too. For this purpose, the HTWG Konstanz campus was chosen as testing site. It is surrounded by high buildings and many trees are close to the chosen track which is depicted in figure 3. The same radio controlled model car that was used in the dynamic test was employed here.

Fig. 3. HTWG Konstanz campus with the estimated reference track in red (source: Microsoft Bing Maps[TM])

Because we did not have a reference system to obtain the rover's true position, we can only present an estimation of the driven track.

First, we applied the generic white noise model with $\sigma = 100m$ as process error. Figure 4 shows the position jumps that occur in the eastern part of the campus, where the nearby buildings obscure the view to most of the received satellites. Many cycle slips and complete losses of lock lead to reinitialization of the ambiguities N' with the pseudorange observations (see section 2.2.1). The pseudorange observations are biased by heavy multipath effects in this case, resulting in severe jumps in the calculated positions.
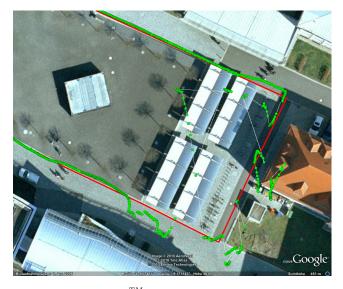

Fig. 4. Google Earth[TM] position plot of HTWG campus test. Q_t as white noise with $\sigma = 100m$. Red: estimated reference track; green: computed positions

In order to reduce the jumps in the position output, we applied a different model for the process error Q_t. Because the radio controlled model car nearly does not move vertically, it makes sense to assign a small σ value to vertical movement. Furthermore, horizontal movements are limited to the maximum velocity of the RC car. The result was a random walk model with process spectral density $\frac{\Delta\sigma^2}{\Delta t} = 1\frac{m^2}{s}$ for the horizontal component and $\frac{\Delta\sigma^2}{\Delta t} = 0.05\frac{m^2}{s}$ for the vertical component. As expected, this limits the position jumps because the Kalman filter now estimates slower movements and weights the erroneous observations less than before. This can be seen in figure 5.
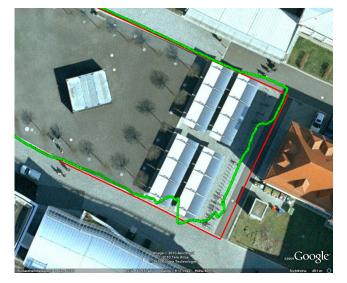

Fig. 5. Google Earth™ position plot of HTWG campus test. Q_t as random walk with horizontal $\frac{\Delta\sigma^2}{\Delta t} = 1\frac{m^2}{s}$ and vertical $\frac{\Delta\sigma^2}{\Delta t} = 0.05\frac{m^2}{s}$. Red: estimated reference track; green: computed positions

The downside of this modification is, however, that the random walk model needs to be tuned carefully to the kinematic characteristics of the rover. If the $\frac{\Delta\sigma^2}{\Delta t}$ values are too small, the positions tend to drift away and do not converge to the true position anymore. On the other hand, too big values do not limit the position jumps sufficiently. A sensor fusion with the robot's odometer sensors could solve this problem in a better way. The odometer information could be used as control input to the Kalman filter.

4. CONCLUSION

In this paper we presented the development of a differential GPS system for the use in mobile robotics environments. In contrast to already existing RTK solutions which use expensive geodetic grade double frequency receivers, our goal was to keep costs minimal. By utilizing the carrier phase observations and benefiting from short baselines, the developed approach provides a positioning accuracy that should be sufficient for many desirable applications. Problems occurred under bad receiving conditions, for example when high buildings caused cycle slips or complete losses of lock. We were able to reduce the resulting jumps in the position output partially by modeling the process

noise as random walk instead of white noise. Thereby, we applied different models for horizontal and vertical movement and adjusted them to the kinematic characteristics of our robot. By fusing the robot's odometer sensors with the Kalman filter presented in this paper, we expect an effective reduction of these jumps. Finally, only more high quality sensor information allows to enhance accuracy. We will investigate this approach in future work.

REFERENCES

Gander, W., Golub, G.H., and Strebel, R. (1994). Least-squares fitting of circles and ellipses. *BIT*, 43.

Gao, Y. (2006). What is precise point positioning (ppp), and what are its requirements, advantages and challenges? *InsideGNSS*, 1(8), 16–18.

Liu, J., Cannon, M.E., Alves, P., Petovello, M.G., Lachapelle, G., MacGougan, G., and deGroot, L. (2003). A performance comparison of single and dual frequency GPS ambiguity resolution strategies . *GPS Solutions*, 7(2), 87–100.

Odijk, D., Traugott, J., Sachs, G., Montenbruck, O., and Tiberius, C. (2007). Two approaches to precise kinematic gps positioning with miniaturized l1 re ceivers. In *Proceedings of ION GNSS 20th International Technical Meeting of the Satellite Division*, 827–838. The Institute of Navigation, Fort Worth, TX.

Pinchin, J., Hide, C., Park, D., and XiaoQi, C. (2008). Precise kinematic positioning using single frequency GPS receivers and an integer ambiguity constraint. In *Position, Location and Navigation Symposium, 2008 IEEE/ION*, 600–605.

Salazar, D., Hernandez-Pajares, M., Juan, J., and Sanz, J. (2008). High accuracy positioning using carrier-phases with the open source GPSTk software. In *Proceedings of the 4th. ESA Workshop on Satellite Navigation User Equipment Technologies*. NAVITEC 2008, Noordwijk, The Netherlands.

Takasu, T. and Yasuda, A. (2008). Evaluation of RTK-GPS Performance with Low-cost Single-frequency GPS Receivers . In *Proceedings of International Symposium on GPS/GNSS 2008*. Tokyo, Japan.

Tolman, B., Harris, R.B., Gaussiran, T., Munton, D., Little, J., Mach, R., Nelsen, S., and Renfro, B. (2004). The GPS Toolkit: Open Source GPS Software. In *Proceedings of the 16th International Technical Meeting of the Satellite Division of the Institute of Navigation*. Long Beach, California.

Welch, G. and Bishop, G. (1995). An Introduction to the Kalman Filter. Technical report, Chapel Hill, NC, USA.